

Nonequilibrium relaxation study of Ising spin glass models

Yukiyasu Ozeki

Department of Physics, Tokyo Institute of Technology, Oh-okayama, Meguro-ku, Tokyo 152-8551, Japan

Nobuyasu Ito

Department of Applied Physics, School of Engineering, The Tokyo University, Bunkyo-ku, Hongo, Tokyo 113-8656, Japan

(Received 22 September 1999; revised manuscript received 24 January 2000; published 20 June 2001)

As an analysis of equilibrium phase transitions, the nonequilibrium relaxation method is extended to the spin glass (SG) transition. The $\pm J$ Ising SG model is analyzed for three-dimensional (cubic) lattices up to the linear size of $L=127$ and for four-dimensional (hypercubic) lattice up to $L=41$. These sizes of systems are quite large as compared with those calculated, so far, by equilibrium simulations. As a dynamical order parameter, we calculate the clone correlation function (CCF) $Q(t, t_w) \equiv [\langle S_i^{(1)}(t+t_w) S_i^{(2)}(t+t_w) \rangle^F]$, which is a spin correlation of two replicas produced after the waiting time t_w from a simple starting state. It is found that the CCF shows an exponential decay in the paramagnetic phase, and a power-law decay after aginglike development ($t \gg t_w$) in the SG phase. This provides a reliable upper bound of the transition temperature T_g . It is also found that a scaling relation, $Q(t, t_w) = t_w^{-\lambda} \bar{q}(t/t_w)$, holds just around the transition point providing the lower bound of T_g . Together with these two bounds, we propose a new dynamical way for the estimation of T_g from much larger systems. In the SG phase, the power-law behavior of the CCF for $t \gg t_w$ suggests that the SG phase in short-range Ising models has a rugged phase space.

DOI: 10.1103/PhysRevB.64.024416

PACS number(s): 75.50.Lk, 05.70.Ln, 05.10.-a

I. INTRODUCTION

The picture of the spin glass (SG) phase is established in the mean-field level^{1,2} based on the replica symmetry breaking (RSB).³⁻⁵ It is characterized by the multivalley structure of the free-energy landscape in the order-parameter space with the so-called ultrametric structure. Since the upper critical dimensions of the SG systems are large, such a mean-field picture might be improper in some physical situations. Studies on the short-range SG model have played an important role to interpret and understand the experimentally observed SG phenomena. Now the lower critical dimensions of the SG transitions and the validity of the RSB picture in short-range SG models are the important remaining problems. Since randomness and frustration make it difficult to treat short-range SG models analytically, as well as numerically, many efforts have been devoted to overcome it in the last two decades.

In the middle of 1980's, some extensive and efficient Monte Carlo simulations were presented for the $\pm J$ Ising model in three dimensions.⁶⁻⁸ The equilibrium quantities relevant to SG transitions were estimated to conclude the existence of the SG phase. The estimated transition temperature, $T_g = 1.175 \sim 1.2$ in units of J/k_B , was consistent with that obtained by series expansion,⁹ providing the confirmation of the equilibrium SG transition in three dimensions. With all such studies, the problems have remained unsettled because of frustration and randomness. The recent result obtained by Monte Carlo simulation in equilibrium states¹⁰ with the same strategy as in Ref. 6 shows a slightly lower value of the SG transition temperature $T_g = 1.11(4)$. It also changes the physical picture of the SG phase in three dimensions; a Kosterlitz-Thouless-like marginal phase¹¹ was suggested in Ref. 6, while a finite SG ordering is suggested in Ref. 10. The main advantage of the simulation in Ref. 10 to that in

Ref. 6 is the amount of calculations that are spent to increase the system size from 16^3 to 24^3 and to lower the temperature range from $T \geq 1.0$ to $T \geq 0.95$. As stated in Ref. 10, these problems are still unsettled, and further investigations are necessary. However, because of the slow relaxation in the SG system, equilibration and averaging takes much time in standard equilibrium Monte Carlo simulations. Larger systems are much difficult to simulate.

Slow dynamics is one of the peculiar properties characterizing the SG phase.^{5,12-19} A typical realization of slow dynamics is the so-called "aging":¹³⁻¹⁷ The relaxation behavior depends strongly on the waiting time from which the environment of the system is changed. Since the equilibration time in real SG materials would be longer than the observation time, the SG phenomena observed in experiments are in a nonequilibrium relaxation process to the equilibrium state. While direct analysis for the equilibrium state has been a main part of the SG theory to show that the phenomenon is a kind of thermodynamic phase transition, analysis for nonequilibrium relaxation is also an important step to understand the SG. Recent progress on the theory of SG is partly owing to studies on nonequilibrium phenomena.¹⁵⁻²⁰

The study of the nonequilibrium relaxation (NER) process is shown to be useful to analyze the equilibrium phase diagram and the critical phenomena.²¹⁻²⁹ It was first applied to the study on ferromagnetic (FM) transitions to estimate the critical point and the dynamic critical exponent quite accurately. One may simulate the relaxation process from the all-up state and measure the total magnetization $m(t)$. The statistical average is taken from independent Monte Carlo runs. In the nonequilibrium process, simulation steps for equilibration are not necessary, and therefore we can treat large systems for which the equilibrium simulation is unreachable.

In the present paper, we show the applicability of the

NER method to SG transitions. In the NER analysis of SG systems, the difficulties that restrict possible system sizes in equilibrium Monte Carlo studies, become milder, and one may simulate much larger systems. Further, since the statistical averaging is taken from independent samples, it is easy to eliminate the systematic bias, which is likely to mislead the conclusions of simulation study. In spite of such advantages for the NER method, two problems arise to extend it to the SG case. One is how to prepare a good initial, nonequilibrium state, which is the all-up state in the FM case. The other is what the good dynamical order parameter is instead of the magnetization. These problems correspond to the question of the proper static order parameter for the equilibrium SG phase. One answer to this question is the replica overlap, and the clone correlation function (CCF)^{6,16–19} is adopted here. It measures the spin correlation between real replicas produced after the relaxation for a waiting time t_w from the all-up state. We investigate the behavior of the CCF for the $\pm J$ Ising SG model in three and four dimensions. The linear sizes simulated are up to $L=127$ with times $t_w \leq 10^8$ and $t \leq 2 \times 10^8$ MCS in three dimensions and $L=41$ in four dimensions. It has been found that the asymptotic behavior of the CCF and the scaling behavior around $t=t_w$ provide a new dynamical way for the estimation of the SG transition temperature, which is more reliable with much larger sizes. It is shown that the asymptotic behavior of the CCF in the SG phase is quite different from that in the FM phase. This indicates a complex phase space like in the mean-field model.

The organization of this paper is as follows. In the next section, the basic idea of the NER method is described for the FM case, and the CCF is introduced for the SG case. Several candidates for the NER function are examined. In Sec. III, the basic properties of the CCF are investigated numerically for the $\pm J$ Ising model in three dimensions. Two time regimes $t > t_w$ and $t < t_w$, and three temperature regimes $T > T_g$, $T \sim T_g$, and $T < T_g$ are distinguished. The asymptotic behavior of the CCF is investigated for several systems in Sec. IV to clarify the usefulness of the NER analysis to the SG case. It reveals the structure of the free energy in the SG phase. In Sec. V, the determination of the transition temperature from numerically obtained CCF, is discussed. The last section is devoted to summary and remarks.

II. NONEQUILIBRIUM RELAXATION METHOD AND SPIN GLASS PHASE

We study the $\pm J$ Ising model mainly on the simple cubic lattice with the interaction energy

$$\mathcal{H} = - \sum_{\langle i,j \rangle} J_{ij} S_i S_j \quad (S_i = \pm 1), \quad (2.1)$$

where the sum runs over all nearest-neighbor sites. The quenched coupling constant J_{ij} takes $J(>0)$ with probability p , or $-J$ with probability $(1-p)$. We study only the symmetric case ($p=1/2$) in this paper. In the following, we use J/k_B as the unit of temperature. The SG transition temperature is expected around $1.11 \leq T_g \leq 1.2$.^{6–10}

The analysis by the NER method is simple and efficient for conventional critical phenomena in equilibrium. In the case of FM transitions, one may simulate the relaxation process from the completely ordered state, i.e., the all-up state, and measure the magnetization $m(t)$. In the relaxation of $m(t)$, the power-law asymptotic behavior

$$m(t) \sim t^{-\lambda_m} \quad (2.2)$$

appears only at the critical point. The magnetization decays exponentially in time to zero in the paramagnetic (PM) phase, and to a positive spontaneous-magnetization value in the FM phase. One of the two ordered states is selected as the initial nonequilibrium state. Note that it is not necessary to select the completely ordered state as the initial state. A state that contains one ordering more than the other is sufficient. As is shown later in Fig. 5, even a random initial configuration works if the CCF is observed instead of the magnetization.

The phase is distinguished by examining the behavior of $m(t)$. If one assumes the dynamic scaling form,^{30,31}

$$m(t, \varepsilon, L) = L^{-\beta/\nu} g(L^{1/\nu} \varepsilon, L^{-z} t), \quad (2.3)$$

where L is the linear size and $\varepsilon \equiv |T - T_c|/T_c$, the power in Eq. (2.2) is related to conventional static and dynamic critical exponents as

$$\lambda_m = \frac{\beta}{z\nu}. \quad (2.4)$$

To distinguish the phase accurately from the data, it is convenient to define the local exponent $\lambda(t)$ by the logarithmic derivative of $m(t)$

$$\lambda(t) \equiv - \frac{d \log m(t)}{d \log t}. \quad (2.5)$$

It approaches to λ_m asymptotically ($t \rightarrow \infty$) at the critical temperature, while it approaches to 0 and ∞ in FM and PM phases, respectively. Therefore, one can determine the critical temperature as the point where $\lambda(t)$ changes its behavior in the $1/t \rightarrow 0$ limit. The finite-time correction for $\lambda(t)$ is of the same order as the correction in $m(t)$. For example, if one assumes

$$m(t) = t^{-\lambda_m} [a_m + O(1/t)] \quad (2.6)$$

at the critical temperature

$$\lambda(t) = \lambda + O(1/t) \quad (2.7)$$

is satisfied. At the critical point, the correction term $O(1/t)$ would be of the order of $1/t^{\omega_m}$ ($\omega_m > 0$). In this sense, the asymptotic behavior of $\lambda(t)$ can be determined easily. In the NER analysis, the error bar of the transition temperature is estimated directly from asymptotic behaviors indicated out of criticality; the upper bound for T_c is the lowest temperature indicating $\lambda(t) \rightarrow \infty$, and the lower bound is the highest temperature indicating $\lambda(t) \rightarrow 0$. Such an estimation of error bars is much more reliable compared with those obtained by conventional scaling-plot analysis.

In general, the correlation length $\xi(t)$ is growing in the nonequilibrium process from zero at the initial state up to the equilibrium value $\xi_{\text{eq}}(T)$. In the region far from the criticality, where $\xi_{\text{eq}}(T) < L$ holds, the relation $\xi(t) < L$ is always satisfied and the nonequilibrium process reflects the behavior of the system in the thermodynamic limit. In the critical region, where $\xi_{\text{eq}}(T) > L$, the characteristic time defined by $\xi(\tau_L) \sim L$ exists. The finite-size effect is observed for $t > \tau_L$. Thus the analysis of nonequilibrium relaxation should be reliable only up to the time much smaller than this τ_L . Since simulation steps for equilibration are not necessary in the NER method, one can treat large systems for which the equilibrium simulation is unreachable. One can simulate systems with large enough τ_L to analyze the thermodynamic behavior sufficiently from the nonequilibrium relaxation for $t < \tau_L$.

Since equilibration takes a very long time for SG systems, the equilibrium simulation suffers from many troubles. In a recent study, the simple-cubic lattice of the size 24^3 was equilibrated by a standard Monte Carlo simulation.¹⁰ As stated above, large systems can be analyzed by the NER method, and the characteristic time τ_L is expected to be large at the transition point even in the SG case. In the present paper, we analyze the equilibrium properties of the $\pm J$ Ising model with sizes up to $127^2 \times 128$ in three dimensions.

In the SG case, unlike in the FM case, the initial state is difficult to be adjusted to the complete ordering and it is nontrivial to define the order-parameter dynamically. In the present paper, we try to apply the method using the CCF (Refs. 6,16–19) $Q(t, t_w)$. Let us consider a system relaxed in a heat bath of temperature T for time interval t_w from the all-up state. This state is recognized as the initial state (at $t = 0$) of the observation. Then, we generate two replicated systems ($S^{(1)}$ and $S^{(2)}$) and simulate them in the same heat bath independently, applying independent random-number sequences. The spin states of these replicas at the i th site after time interval t from the initial state, are denoted by $S_i^{(1)}(t+t_w)$ and $S_i^{(2)}(t+t_w)$. The overlap of these two replicas

$$Q(t, t_w) \equiv [\langle S_i^{(1)}(t+t_w) S_i^{(2)}(t+t_w) \rangle^F], \quad (2.8)$$

is estimated at each time step, where $\langle \dots \rangle^F$ and $[\dots]$ represent the dynamical average in the above process and the average for bond randomness, respectively. We call the state at the beginning of the waiting, which is the all-up one, the starting state, and that at the end of the waiting, the initial state, hereafter. It is noted that the all-up state is not special in the SG case. The dynamics in this process is equivalent to that from a complete random state at least for the $p = 1/2$ case. Similar relations were widely proven for any p (the aging relation).^{32,33} Thus, one may consider that $Q(t, t_w)$ is the CCF with a complete random state as the starting state. This means that the starting state contains all the thermodynamic states equally even in the SG phase.

At the initial state ($t = 0$), the CCF is equal to unity, the maximum value. During the waiting time t_w between the starting and initial states, the SG ordering develops to some extent in the SG phase and some thermodynamic states have

larger amplitudes than the others in the initial state. The SG ordering is still incomplete in the initial state. Only in the $t_w \rightarrow \infty$ limit, the complete ordering is expected. Therefore, the behavior of the CCF depends on the waiting time in the SG phase. If the initial state is in equilibrium, which can be achieved by $t_w \rightarrow \infty$, the CCF approaches the SG order parameter asymptotically. When $t_w < \infty$, the asymptotic behavior of the CCF will be clarified later.

We define the local exponent of $Q(t, t_w)$ as

$$\lambda(t, t_w) \equiv - \frac{d \log Q(t, t_w)}{d \log t}, \quad (2.9)$$

to analyze the asymptotic behavior more precisely. Practically, the local exponent $\lambda(t, t_w)$ is estimated by the least-square fitting of $\log Q(t, t_w)$ to $\log t$ in a finite interval $t - \Delta t < t' < t + \Delta t$, where Δt ($\ll t$) is chosen appropriately.

The well-defined asymptotic behavior (large t behavior) for the CCF is achieved by $t_w \rightarrow \infty$, in which the SG order parameter is obtained asymptotically. Although large systems with large τ_L are simulated, it is impossible to analyze the limit of $t_w \rightarrow \infty$ from the CCF, since the finite-size effect occurs for $t + t_w > \tau_L$. This makes the analysis complicated and unreliable compared with the results obtained from $t + t_w < \tau_L$. Thus, we need to examine whether or not the CCF gives relevant information for the SG transition even in $t + t_w < \tau_L$. In this case, the asymptotic (large t) behavior is observed in the regime $\tau_L > t \gg t_w$; the regime $\tau_L > t_w \gg t \gg 1$ is difficult to be simulated in general.

Before showing the numerical results, we examine other candidates for the order parameter, which we do not use for the following reasons. In any case, the initial state cannot be chosen perfectly appropriately, since the ordered state in the SG phase is nontrivial and is unknown before simulation. The simplest quantity in the study of magnetism is the magnetization

$$m(t) \equiv [\langle S_i(t) \rangle^{\text{ne}}], \quad (2.10)$$

where $\langle \dots \rangle^{\text{ne}}$ represents the dynamical average in a nonequilibrium process, while it has several problems in the application to the SG case. Since the complete state (all-up), which gives the maximum value of $m(t)$, has zero overlap to the SG states, we are not sure whether or not it is relevant to the SG ordering. It always vanishes in equilibrium states in zero field. This suggests a difficulty distinguishing the phase from the asymptotic behavior. The amplitude of $m(t)$ in the SG phase is much smaller compared with the FM case. Thus, we discard this possibility.

The equilibrium autocorrelation function

$$q(t) \equiv [\langle S_i(0) S_i(t) \rangle^{\text{eq}}], \quad (2.11)$$

where $\langle \dots \rangle^{\text{eq}}$ represents the dynamical average in the equilibrium process, approaches the SG order parameter asymptotically. However, this quantity is not suitable for our purpose, since it is required to generate equilibrium states before relaxations, which limits the system size.

The nonequilibrium autocorrelation function

$$C(t, t_w) \equiv [\langle S_i(t_w) S_i(t+t_w) \rangle^{\text{ne}}] \quad (2.12)$$

does not need the equilibration. This is more suitable than those listed above. It has been observed that $C(t, t_w)$ depends on the waiting time t_w (the aging phenomena), and the crossover appears around $t \sim t_w$.¹⁵ Before the crossover ($t < t_w$), it behaves as in equilibrium since the state at time t_w approaches the equilibrium state when $t_w \rightarrow \infty$. In the asymptotic regime, $C(t, t_w)$ decays to zero even in the SG phase. Practically, the stack of spin configurations needs much memory space or it restricts the observation steps. To avoid this stack problem, similar to $C(t, t_w)$ but with more practical quantity, the CCF is proposed.

III. NUMERICAL RESULTS

In this section, we report the behavior of the CCF estimated by Monte Carlo simulations. In the simulations, single-spin flip dynamics with two-sublattice updates have been used.³⁴ Simple-cubic lattices with sizes from $29^2 \times 30$ up to $127^2 \times 128$ have been simulated. The simulations were performed for temperatures in the range $0.8 \leq T \leq 2.2$ with times up to $t_w = 10^8$ and $t = 2 \times 10^8$. To achieve maximum simulation performance, skew boundary conditions were imposed for two directions, and the remaining direction is periodic. With this boundary condition, our two-sublattice vectorization simulation requires the lattice size of (odd) \times (odd) \times (even). The size dependence is checked for several sizes and it is confirmed that these lattices are large enough to eliminate the finite-size effects up to the present maximum time of simulations within the present accuracy.^{35–40} Typical lattices are $63^2 \times 64$ and $101^2 \times 102$. For simulations longer than the order of 10^7 Monte Carlo steps (MCS), smaller lattices, $29^2 \times 30$, $39^2 \times 40$ and $49^2 \times 50$, have been analyzed. Even these smaller lattices are much larger than those calculated so far in equilibrium Monte Carlo simulations. The number of independent bond configurations N_b is chosen from tens to thousands for each temperature T .

The typical behavior of the CCF is shown in Figs. 1(a)–1(c). In the PM phase [Fig. 1(a)], $Q(t, t_w)$ shows an exponential decay in time t .⁴¹ The decay time is called the thermalization time and denoted by τ . It does not depend on the waiting time t_w but on the temperature T for large t_w . It is observed that $Q(t, t_w)$ shows t_w dependence if $t_w < \tau$, while it is independent of t_w if $t_w > \tau$. When $t_w > \tau$, the starting state relaxes during the waiting time and the initial state reaches an equilibrium state, so $Q(t, t_w)$ shows equilibrium replica-spin relaxation. On the other hand, when $t_w < \tau$, the initial state is not an equilibrium state and depends on t_w . Therefore, the CCF involves two time scales, τ and t_w , in the PM phase. The values of τ are estimated by the least-square fitting for $T > T_g$, and are plotted in Fig. 2. The figure shows a power-law divergence on $(T - T_g)$, in which $T_g = 1.2$ is assumed. The exponent is estimated as $z\nu = 5.7(5)$. This value is smaller than previous estimations, $z\nu = 6.5 \pm 1.5$ in Ref. 6, $z\nu = 6 \pm 1$ in Ref. 7, and $z\nu = 7.2 \pm 1$ in Ref. 8, but is not very distinct from them.

At a temperature close to the critical point [Fig. 1(b), $T = 1.2$] or in the SG phase [Fig. 1(c), $T = 0.9$], $Q(t, t_w)$ shows a power-law decay in time t and the amplitude depends on

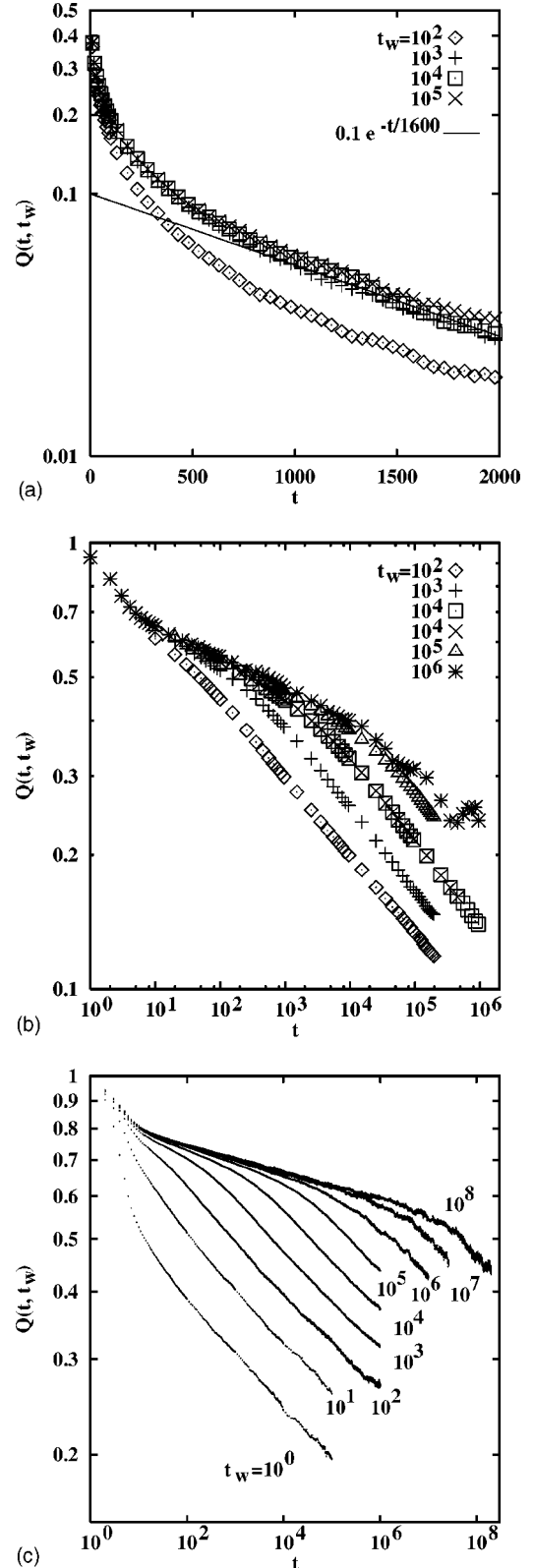


FIG. 1. Behavior of the CCF is shown for the simple-cubic lattice of several temperatures, (a) $T = 1.6$, (b) $T = 1.2$, and (c) $T = 0.9$. The solid line in (a) is shown as a guide to the eyes to give an idea of the relaxation time scale. Figure (a) is a semilog plot, and (b) and (c) are double-log plots.

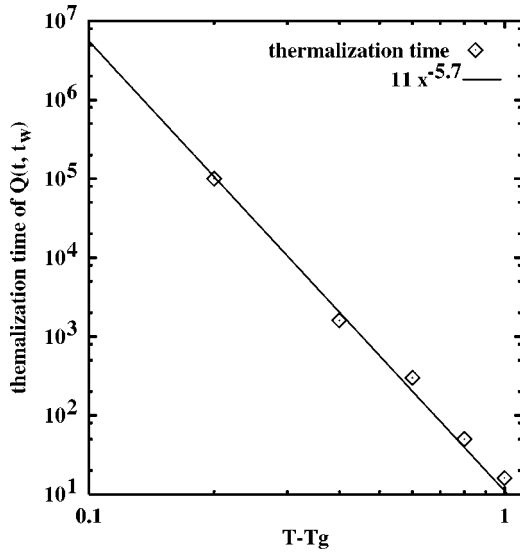


FIG. 2. Behavior of the thermalization time in the PM phase is shown for the simple-cubic lattice. $T_g = 1.2$ is assumed.

t_w . The waiting time dependence is clearly observed and it gives the time scale of dynamical behavior: A crossover is found from one power law to the other at around $t \sim t_w$. In the regime of $t \ll t_w$, $Q(t, t_w)$ will not depend on t_w if t_w is large enough, while it does in the asymptotic regime $t \gg t_w$. The decay exponent for $t \gg t_w$ seems to be independent of t_w . Such a crossover appears in a wide range of temperature below T_g . This is a part of aging phenomena characteristic of SG systems.^{13–15}

To see the dynamical behavior more clearly, we estimate the local exponent $\lambda(t, t_w)$ and plot it as a function of logarithmic-scaled t_w/t in Figs. 3(a)–3(c), in which the behavior in whole time regime, especially around the crossover regime, can be seen. First, we examine the asymptotic behavior in the regime $t \gg t_w$. In this regime, the CCF describes a nonequilibrium relaxation, essentially. Let us see Fig. 3(a) for the high-temperature region ($T > T_g$). The local exponents for all waiting times are rapidly increasing with t at around $1/t = 0$. From the standard NER analysis,^{23–29} this indicates the divergence of $\lambda(t, t_w)$ as $t \rightarrow \infty$ and the relaxation faster than a power law, possibly an exponential law in the PM phase as it is also observed directly in Fig. 1(a). For $T \leq T_g$, the local exponent approaches a definite value independent of the waiting time. This is observed as the saturation in small t_w/t in Figs. 3(b)–3(c). The power becomes smaller when the temperature is lower.⁴³ Further consideration for the regime $t \gg t_w$ is given in the following sections.

In the regime of $t \ll t_w$, the CCF is considered to converge to the equilibrium value of replica spin overlap when $t_w \rightarrow \infty$, since the initial state approaches the equilibrium state. It is observed that the waiting-time dependence of the local exponent with fixed $t_w/t \gg 1$ changes around the transition temperature in this regime. It is increasing with t_w for $T > T_g$ [see Fig. 3(a)] while decreasing for $T < T_g$ [see Fig. 3(c)].⁴⁴ In the limit of $t_w \rightarrow \infty$, if $\lambda(t, t_w)$ diverges for $T > T_g$, it is consistent with the exponential decay for the PM phase or nonexponential but faster than a power-law decay

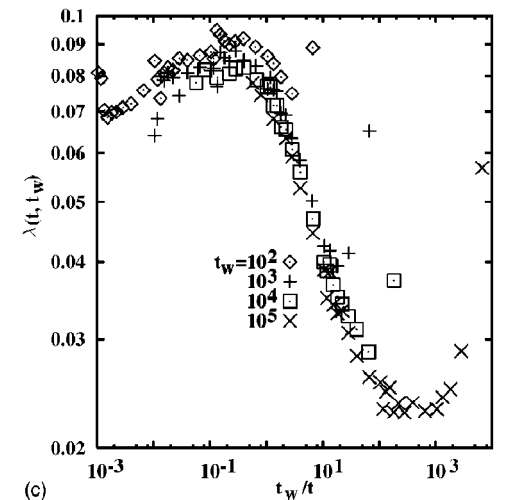
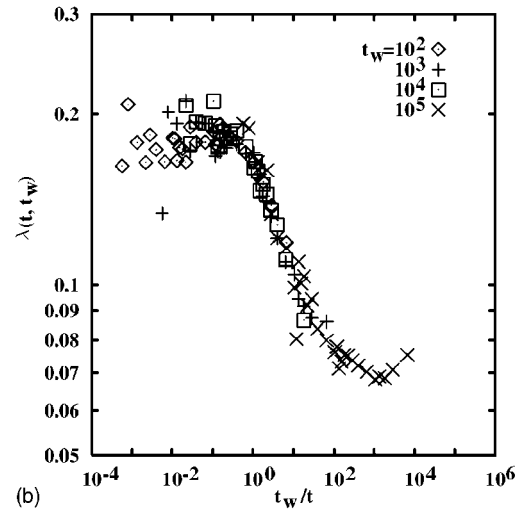
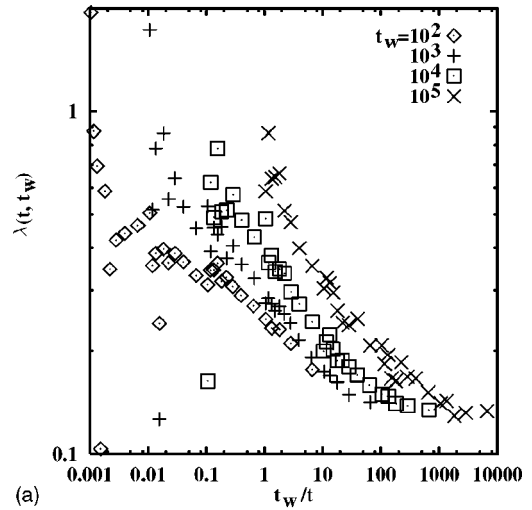


FIG. 3. Local exponents of the CCF in three dimensions are plotted as functions of t_w/t . The horizontal axis is in the logarithmic scale. The temperatures are (a) $T = 1.4$, (b) $T = 1.2$, and (c) $T = 0.8$.

for the Griffiths phase in equilibrium relaxation.^{8,12,42} If $\lambda(t, t_w)$ vanishes for $T < T_g$, there exists a finite SG ordering in the equilibrium state. Around the critical point, the local exponent $\lambda(t, t_w)$ is waiting-time independent as a function

TABLE I. The behavior of the CCF for each temperature region. Two time regimes, $t < t_w$ and $t > t_w$, are distinguished. The asymptotic form of the CCF and the waiting-time dependence of $\lambda(t, t_w)$ with t_w/t fixed are listed.

Temperature	$T < T_g$	$T = T_g$	$T > T_g$
$t < t_w$			
Asymptotic form	Finite order	Power	Exponential
t_w dep. of $\lambda(t, t_w)$	decreasing	constant	increasing
$t > t_w$			
Asymptotic form	Power	Power	Exponential
t_w dep. of $\lambda(t, t_w)$	constant	constant	increasing

of t_w/t , indicating the equilibrium critical relaxation. The behavior of the CCF for each temperature regions is summarized in Table I.

In the present simulation, the waiting-time dependence still remains even for the largest waiting time [see Fig. 1(c)]. That means the largest waiting time, 10^8 MCS, is insufficient for equilibration in the SG phase.

IV. ASYMPTOTIC BEHAVIOR IN THE SPIN GLASS PHASE

In this section, we discuss the asymptotic behavior ($t \gg t_w$) of the CCF in the SG phase from the present data to examine the applicability of the NER analysis to SG transitions. In three dimensions, the CCF in the SG phase decays algebraically with a power independent of the waiting time [see Figs. 1(c) and 3(c)]. Two possibilities can be considered to interpret it. One is that the SG phase in three dimensions is of the Kosterlitz-Thouless type,^{6,11} in which no finite order parameter appears while the spatial correlation length always diverges. The other possibility is that the CCF has a character that asymptotically approaches zero in the SG phase even when there exists a finite SG ordering.

To show that the latter is the case, we calculate the CCF for the $\pm J$ Ising model in four dimensions (see Fig. 4), in which a finite SG ordering is widely expected^{6,9} below $T_g(4D) \sim 2.0$. Calculations are performed at $T = 1.2$ on the four-dimensional hypercubic lattice with sizes up to $41^3 \times 42$. The number of independent bond configurations N_b is taken to be 32. We observe a crossover behavior from one power-law decay to another at around $t \sim t_w$. In the $t < t_w$ regime, the power depends on t_w , while it seems independent of t_w in the asymptotic regime $t \gg t_w$. These behaviors are the same as in the observation in three dimensions. Since the SG phase in four dimensions has a finite SG ordering, we conclude that the CCF has the character of a power-law decay in the SG phase in any dimensions and does not converge to any finite values. Even though the CCF does not approach the equilibrium order parameter, the relaxation behavior is useful to analyze the equilibrium properties, which will discuss later.

What is the physical origin of this nonequilibrium relaxation? To clarify it, we compare the behavior in the SG phase with a simpler case, the CCF in the pure FM model

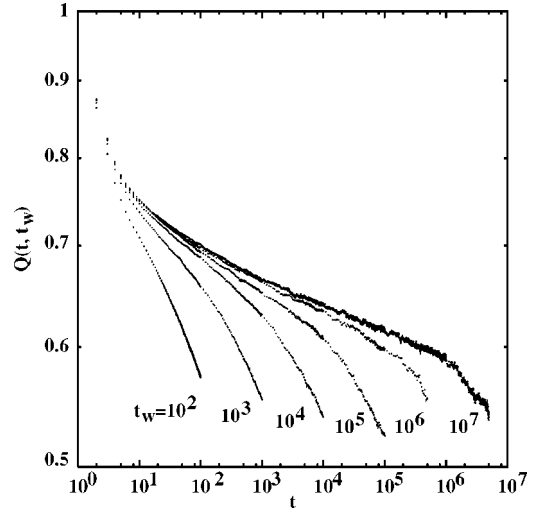


FIG. 4. CCF in the SG phase ($T = 1.2$) in four dimensions. The transition temperature is estimated around $T_g \sim 2.0$, (Refs. 6 and 9) and finite SG ordering is expected at $T = 1.2$. The waiting time t_w is varied from 10^2 to 10^7 . The waiting-time dependence and the crossover behavior around $t \sim t_w$ are observed.

from a random starting state at $T < T_c$. Calculations have been performed for the three-dimensional pure FM Ising model. The result is shown in Fig. 5. The system is on the simple-cubic lattice with the size of $101^2 \times 102$, and CCF values from typically 1280 independent simulations have been averaged over. We observe that the CCF initially decays, then grows and finally approaches a finite value, which will be the square of the spontaneous magnetization.^{45,46} The minimum occurs at around the same time scale ($t \sim 300$) for all t_w , and the minimum value is smaller for smaller t_w . This is quite different from the SG case. It is noted that the waiting-time dependence remains at the largest t_w in Fig. 5,

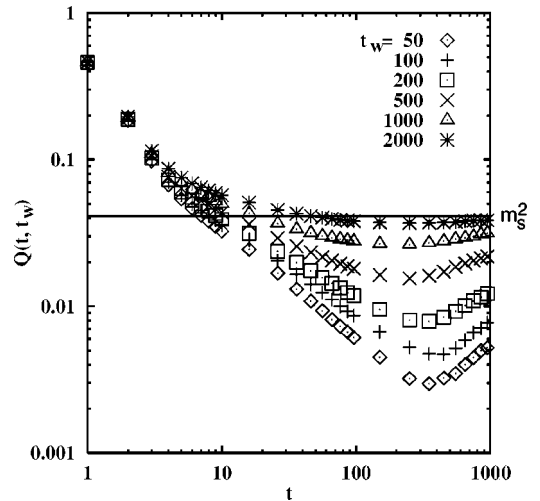


FIG. 5. CCF in the FM phase ($1/T = 0.222$ or $T = 4.505$) for the three-dimensional pure FM Ising model. The transition temperature is $1/T_c = 0.22166$ or $T_c = 0.4511$. The starting state was set to a randomly oriented configuration. The waiting time t_w is varied from 50 to 2000. The horizontal line shows the value of the squared spontaneous magnetization at $1/T = 0.222$.

which means that the initial state is still in nonequilibrium for all t_w . Thus, the observed asymptotic behavior is a non-equilibrium relaxation, which is the same situation as in the present SG calculations.

The minimum of the CCF observed in the FM phase is explained as follows. From the starting random configuration, FM clusters start to grow but the ordering directions are random among clusters. After a while, a few clusters become dominant in the system and they have longer lifetime than other small clusters. The time when the system is occupied by dominant clusters is named the percolating time. The percolated cluster slowly absorbs other nonpercolating clusters (we are assuming the rough FM phase above roughening temperature). When t_w is larger than the thermalization time τ , the initial state is almost at equilibrium and is dominated by a single percolated cluster. Then, the CCF decays monotonically from unity to the equilibrium squared magnetization. On the other hand, when t_w is small enough, the initial state is nonequilibrium and consists only of nonpercolated clusters. Even then, in the initial state, the ordering process has progressed from the starting state and the orientation of the dominant percolated cluster, which will appear in later time, is the same in each replica. Clusters antiparallel to this percolated orientation relax to the opposite direction in time. Since the process to flip such clusters from the initial state is almost independent in two replicas, contributions of them to the CCF are almost negative in early times, and the resulting overlap would decrease to a much smaller value. After a while, flipped clusters begin to correlate with each other in space and time. Then the contributions to the CCF approach those in the equilibrium state.

We examine the difference of asymptotic behaviors of the CCF in FM and SG phases. In general, the ordered phase has more than one pure state. The starting state contains equal dynamical amplitude for each pure state in both FM and SG cases, since it is random. The process in the waiting time provides a domain structure of pure states. In the FM case, even if the process in $t > 0$ is independent, the final equilibrium state is equivalent in two replicas. This means that the dynamical amplitudes of pure states are not equal in the initial state, and only one pure state has a dominant dynamical amplitude relatively. This explains the finite limit of the CCF. In the SG case, the power-law decay of the CCF indicates that the final state is not unique and depends on replica; otherwise the contribution to the CCF must be nonvanishing. This means that the initial state contains more than one pure state with dominant dynamical amplitude, which is different from the FM case. This indicates the complicated structure of the phase space in the short-range Ising SG models, which could be a ultrametric structure like in the Sherrington-Kirkpatrick model.^{2,4}

V. SPIN GLASS TRANSITION AND SCALING RELATION

In the previous sections, we showed the asymptotic behavior of the CCF: it decays exponentially for $T > T_g$, while it shows a power-law decay for $T \leq T_g$, and this decay exponent does not depend on t_w but on T . Thus, we can distinguish the phase by analyzing the asymptotic behavior of the

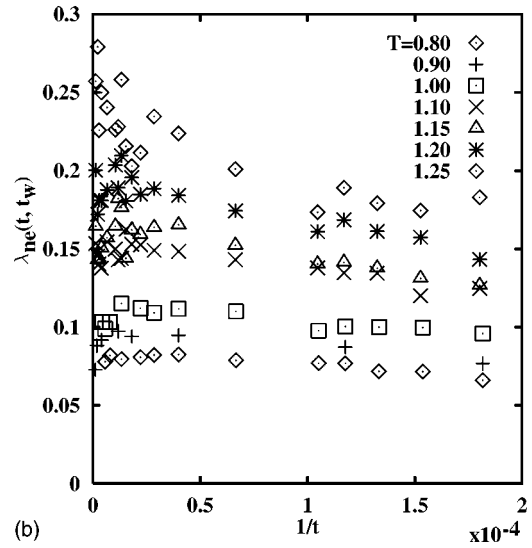
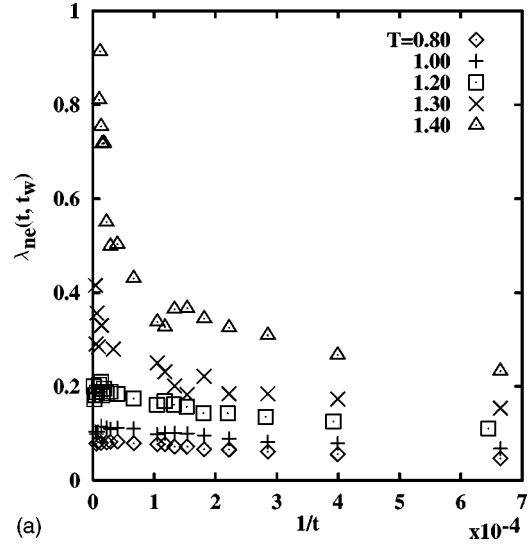


FIG. 6. Local exponents $\lambda_q(t, t_w)$ as functions of $1/t$ with $t_w = 10^4$ fixed. The curves bend upwards as $t \rightarrow \infty$ for $T \geq 1.25$, as expected for the PM phase.

CCF with fixed t_w . For smaller t_w , one can save simulation steps for the waiting time. For larger t_w , the amplitude of the CCF becomes larger, and the statistical deviation is suppressed relatively. An appropriate t_w should be chosen for efficient calculations.

In Fig. 6, we plot the local exponent of $Q(t, t_w)$ for the three-dimensional case with $t_w = 10^4$ (MCS) fixed. It is clearly observed that the curves for $T \geq 1.25$ turn up when $1/t$ goes to zero—indicating the PM phase in this temperature region. This is consistent with the expected transition temperature^{6–10} $1.11 \leq T_g \leq 1.2$. Note that the curves for $T \leq 1.2$ approach nonzero finite values—indicating a power-law decay of $Q(t, t_w)$. This means that the SG transition temperature is located around $T = 1.2$. The temperature $T = 1.25$ is the upper bound of T_g in this analysis, i.e., $T_g < 1.25$.

The above analysis does not give an estimation for the lower bound of T_g , since the downward behavior, which

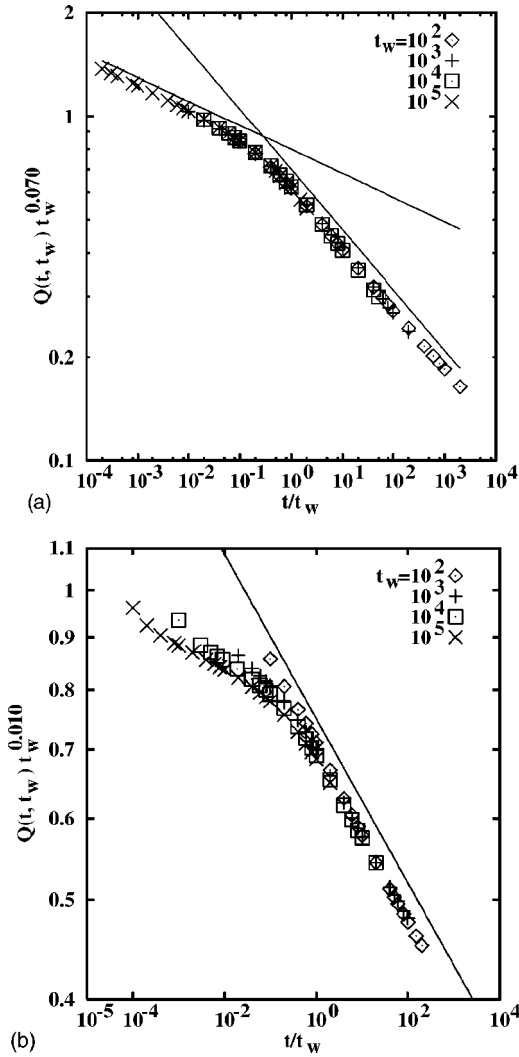


FIG. 7. Scaling plot of $Q(t, t_w)$ at (a) $T=1.20$ and (b) $T=0.8$ in three dimensions. The values of scaling exponent are selected so that the points fall onto the scaling curve for $t/t_w \gg 1$. (a) At $T=1.20$, which is close to the transition temperature, not only the region for $t/t_w \gg 1$, but also that for $t/t_w \ll 1$, are scaled by the single exponent. The solid lines show $a(t/t_w)^{-0.070}$ and $b(t/t_w)^{-0.175}$. These exponents are also observed in Fig. 3(b). (b) At $T=0.80$, only the region $t/t_w \gg 1$ is scaled. The solid line shows $c(t/t_w)^{-0.080}$. This exponent is also observed in Fig. 3(c).

usually means the finite ordering, is not observed for the CCF in the SG phase. The following scaling analysis supplements this problem. At the critical temperature, time scales included in $Q(t, t_w)$ are just t and t_w . Thus, one can expect the scaling form

$$Q(t, t_w) = t_w^{-\lambda_q} \bar{q}(t/t_w), \quad (5.1)$$

which is numerically confirmed for $T=1.2$ in Fig. 7(a) with $\lambda_q=0.070$. This scaling relation is not observed for $T < T_g$. As an example, in Fig. 7(b), we plot $t_w^\lambda Q(t, t_w)$ for $T=0.8$ with λ chosen to fit curves in the regime $t/t_w > 1$; the asymptotic power is t_w independent in this regime. Clearly, curves are spread in $t/t_w < 1$ and the scaling form (5.1) is not

satisfied in the whole t/t_w regime. A similar feature is observed also at $T=1.0$ and 0.9 . Therefore, we conclude that the scaling relation (5.1) is valid only in the critical region near the critical point. The result at $T=1.1$ also shows the scaling form (5.1) both for $t/t_w > 1$ and $t/t_w < 1$. The region $1.1 \leq T \leq 1.2$ is regarded as the critical region within the present simulation. If one estimates the CCF more accurately or for a longer-time interval, higher resolution would be available. It is concluded that $T_g > 1.0$.

At the critical point, the CCF decays algebraically in both limits $t \gg t_w$ and $t \ll t_w$, with powers independent of t_w . Furthermore, the amplitude is also independent of t_w for $t \ll t_w$ because of the convergence to the equilibrium relaxation. That means

$$\bar{q}(x) \rightarrow \begin{cases} \bar{c}_e x^{-\lambda_q} & (x \ll 1) \\ \bar{c}_{ne} x^{-\lambda_{ne}} & (x \gg 1), \end{cases} \quad (5.2)$$

where \bar{c}_e and \bar{c}_{ne} are constants, and $\lambda_q \neq \lambda_{ne}$. Then, the CCF behaves as

$$Q(t, t_w) \rightarrow \begin{cases} \bar{c}_e t^{-\lambda_q} & (t \ll t_w) \\ c_{ne}(t_w) t^{-\lambda_{ne}} & (t \gg t_w), \end{cases} \quad (5.3)$$

where

$$c_{ne}(t_w) = \bar{c}_{ne} t_w^\mu \quad (5.4)$$

with $\mu = \lambda_{ne} - \lambda_q$.⁴⁷ The scaling analysis of the present simulation result provides $\lambda_q = 0.070(5)$ and $\lambda_{ne} = 0.175(5)$ [$\mu = 0.100(5)$] at $T=1.2$ and $\lambda_q = 0.045(5)$ and $\lambda_{ne} = 0.150(5)$ [$\mu = 0.105(5)$] at $T=1.1$. The deviation due to the uncertainty of T_g is more significant than the statistical error. Assuming that T_g is located between 1.1 and 1.2, they are estimated to be $\lambda_q = 0.06(2)$ and $\lambda_{ne} = 0.16(2)$ [$\mu = 0.103(8)$]. The estimated value $\lambda_q = 0.06(2)$ is consistent with those obtained so far by equilibrium simulations.^{8,15,48}

The exponent λ_{ne} characterizes the nonequilibrium relaxation. Huse⁴⁹ observed a power-law decay of the magnetization at the critical point in three dimensions, which would be a nonequilibrium relaxation. The estimated power 0.37 of magnetization is much larger than the present estimation of λ_{ne} for the CCF.

The exponent λ_{ne} can be defined even for $T < T_g$. In the SG phase, the CCF for $t \gg t_w$ behaves as

$$Q(t, t_w) \rightarrow c_{ne}(t_w, T) t^{-\lambda_{ne}(T)}, \quad (5.5)$$

where

$$c_{ne}(t_w, T) = \bar{c}_{ne}(T) t_w^{\mu(T)} \quad (5.6)$$

with $\mu(T) = \lambda_{ne}(T) - \lambda_q(T)$. Estimated values of $\lambda_q(T)$ and $\lambda_{ne}(T)$, from the scaling-plot analysis, are given in Fig. 8. The values of λ_{ne} are also estimated by extrapolation to $1/t = 0$ in Fig. 6, which of course give consistent values from the scaling analysis. Ogielski⁸ gives a figure of $\lambda_q(T)$ from the analysis of the equilibrium autocorrelation function. Our result is consistent with that.

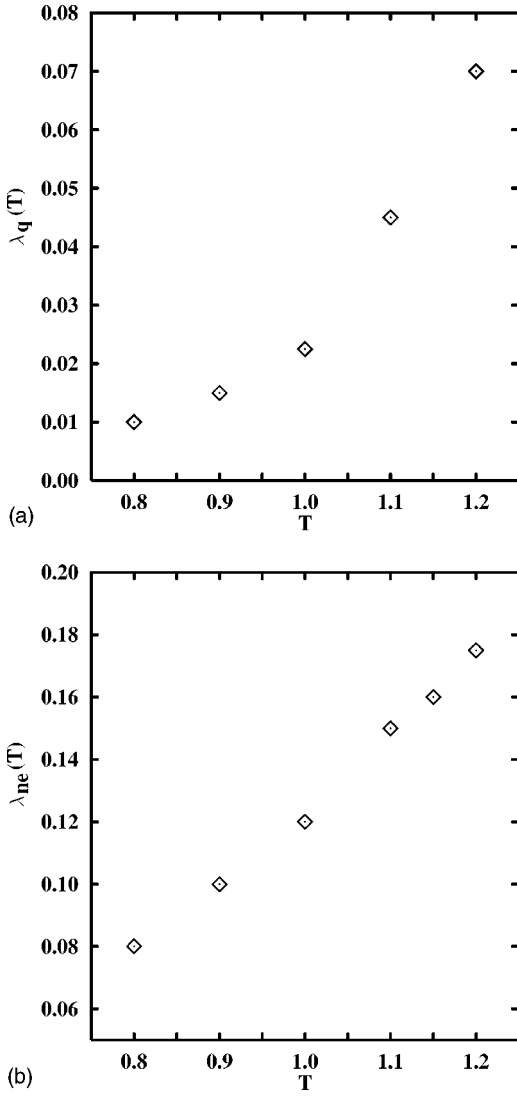


FIG. 8. Temperature dependence of the powers of CCF observed in nonequilibrium relaxation in the SG phase: (a) $\lambda_q(T)$ and (b) $\lambda_{ne}(T)$.

VI. SUMMARY AND REMARKS

The nonequilibrium relaxation method has been extended to analyze SG transitions. The initial state and the dynamical order parameter are nontrivial unlike the FM case. We introduce the CCF, in which the initial state is provided by an appropriate waiting time and the order parameter is estimated by the replica overlap. The behavior of the CCF is investigated for the $\pm J$ Ising model in three-dimensions. The number of totally updated spins for three-dimensional SG simulation is 9.9×10^{15} and it took about 5800 single-processor hours of VPP500. For four-dimensional SG simulation, 1.6×10^{14} spins are updated using about 120 single-processor hours.

It is remarkable that, in the SG phase, the CCF in the region $t \gg t_w$ decays algebraically with a power independent of the waiting time. The CCF in the SG phase is also studied for the four-dimensional $\pm J$ Ising model, which shows qualitatively the same behavior as in three dimensions. These

observations indicate a nontrivial structure of the phase space instead of the double-well type one observed in Fig. 5 for the pure FM model. The behavior of the CCF in the region $t \ll t_w$ in the SG phase, shows the tendency to converge to nonzero positive values, which suggests that the CCF converges to a SG order parameter when t becomes large after taking the limit $t_w \rightarrow \infty$ (i.e., equilibrium relaxation). However even $t_w = 10^8$ is not sufficient to estimate the value of this order parameter at $T = 0.9$.

Although the CCF in the SG phase approaches zero in the asymptotic regime ($t \gg t_w$), it can be useful to analyze equilibrium properties of SG transitions. From the present observation of the CCF, the determination of the transition temperature T_g is possible. In three dimensions, the asymptotic behavior of the local exponent gives $T_g < 1.25$ and the scaling-plot analysis using the form of Eq. (5.1) gives $T_g > 1.0$. At a glance, this result, $1.0 < T_g < 1.25$, is not a precise estimation. However, the studied system sizes $127^2 \times 128$ are much larger than those by equilibrium simulations. Furthermore, this error bar is estimated directly by asymptotic behaviors which indicates out of criticality. Therefore the obtained results have reliability and importance. While the recent estimation¹⁰ of T_g was made carefully, the Binder's cumulant with the finite-size scaling analysis for sizes up to 24^3 , could be modified in the future because of the correction to scaling and the finite-size effect, which was pointed out by the authors of that paper.¹⁰ The present investigation provides another way to estimate for T_g with much larger systems, in which the size effect is not serious.

In three dimensions, the thermalization-time exponent in the PM phase is estimated as $z\nu = 5.7(5)$. The exponents at the critical temperature are $\lambda_q(T_g) = 0.06(2)$ and $\lambda_{ne}(T_g) = 0.16(2)$. The temperature dependence of asymptotic exponents in the SG phase are shown in Fig. 8. The exponent β_q of SG order parameter q is estimated to be $0.34(11)$ assuming the dynamic finite-size scaling relation

$$\lambda_q(T_g) = \frac{\beta_q}{z\nu}, \quad (6.1)$$

with the present estimates for $\lambda_q(T_g)$ and $z\nu$.

The analysis of SG by the CCF is an extension to arbitrary phase transitions especially to those for which the order parameter is not simple. Even with the NER method, such transitions are not easy to treat compared to transitions with a clear order parameter, but the advantage in the system size will still be useful. The present SG analysis will encourage the NER analysis for other complicated systems.

ACKNOWLEDGMENTS

The simulation have been made using the vector-parallel processor Fujitsu VPP500/40 of ISSP (University of Tokyo). The authors thank H. Takayama, I Campbell, S. Miyashita, H. Kawamura, K. Nemoto, K. Hukushima, and H. Yoshino, for fruitful and stimulating discussions. This work is partially supported by the Japan Society for the Promotion of Science No. (10740186).

- ¹S.F. Edwards and P.W. Anderson, *J. Phys. F: Met. Phys.* **5**, 965 (1975).
- ²D. Sherrington and S. Kirkpatrick, *Phys. Rev. Lett.* **35**, 1792 (1975).
- ³K. Binder and A.P. Young, *Rev. Mod. Phys.* **58**, 801 (1986).
- ⁴M. Mézard, G. Parisi, and A. Virasoro, *Spin Glass Theory and Beyond* (World Scientific, Singapore, 1987).
- ⁵K. H. Fischer and J. A. Hertz, *Spin Glasses* (Cambridge University, Cambridge, 1991).
- ⁶R.N. Bhatt and A.P. Young, *Phys. Rev. Lett.* **54**, 924 (1985); *J. Magn. Magn. Mater.* **54-57**, 191 (1986).
- ⁷A.T. Ogielski and I. Morgenstern, *Phys. Rev. Lett.* **54**, 928 (1985).
- ⁸A.T. Ogielski, *Phys. Rev. B* **32**, 7384 (1985).
- ⁹R.R.P. Singh and S. Chakravarty, *Phys. Rev. Lett.* **57**, 245 (1986).
- ¹⁰N. Kawashima and A.P. Young, *Phys. Rev. B* **53**, R484 (1996).
- ¹¹J.M. Kosterlitz and D.J. Thouless, *J. Phys. C* **6**, 1181 (1973).
- ¹²H. Takayama, in *Computational Physics as a New Frontier in Condensed Matter Research* (Physical Society of Japan, Tokyo, 1995), p. 230.
- ¹³L. Lundgren, P. Svedlindh, P. Nordblad, and O. Beckman, *Phys. Rev. Lett.* **51**, 911 (1983).
- ¹⁴E. Vincent, J. Hammann, and M. Ocio, *Recent Progress in Random Magnets*, edited by D. H. Ryan (World Scientific, Singapore, 1992), p. 207.
- ¹⁵H. Rieger, *J. Phys. A* **26**, L615 (1993).
- ¹⁶L.F. Cugliandolo and D.S. Dean, *J. Phys. A* **28**, 4213 (1995).
- ¹⁷A. Barrat, R. Burioni, and M. Mézard, *J. Phys. A* **29**, 1311 (1996).
- ¹⁸A. Baldassarri, cond-mat/9607162; *Phys. Rev. E* **58**, 7047 (1998).
- ¹⁹H. Takayama, H. Yoshino, and K. Hukushima, *J. Phys. A* **30**, 3891 (1997).
- ²⁰E. Marinari, G. Parisi, and F. Zuliani, *J. Phys. A* **31**, 1181 (1998).
- ²¹D. Stauffer, *Physica A* **186**, 197 (1992).
- ²²G.A. Kohring and D. Stauffer, *Int. J. Mod. Phys. C* **C3**, 1165 (1992).
- ²³N. Ito, *Physica A* **192**, 604 (1993).
- ²⁴N. Ito, *Physica A* **196**, 591 (1993).
- ²⁵N. Ito, T. Matsuhisa, and H. Kitatani, *J. Phys. Soc. Jpn.* **67**, 1188 (1998).
- ²⁶Y. Ozeki and N. Ito, *J. Phys. A* **31**, 5451 (1998).
- ²⁷N. Ito, Y. Ozeki, and H. Kitatani, *J. Phys. Soc. Jpn.* **68**, 803 (1999).
- ²⁸N. Ito, K. Hukushima, K. Ogawa, and Y. Ozeki, *J. Phys. Soc. Jpn.* **69**, 1931 (2000).
- ²⁹K. Ogawa and Y. Ozeki, *J. Phys. Soc. Jpn.* **69**, 2808 (2000).
- ³⁰M. Suzuki, *Phys. Lett. A* **58**, 435 (1976).
- ³¹M. Suzuki, *Prog. Theor. Phys.* **58**, 1142 (1977).
- ³²Y. Ozeki, *J. Phys. A* **28**, 3645 (1995).
- ³³Y. Ozeki, *J. Phys.: Condens. Matter* **10**, 11 171 (1997).
- ³⁴An independent-spin coding technique (Refs. 35–37) and shuffling technique (Ref. 38) are applied with Lewis-Payne-type pseudorandom number. (Refs. 39 and 40) The simulations are performed on Fujitsu VPP500/40, each of whose 40 processors has 1.6 GFLOPS peak performance, and the typical performance for simple-cubic lattice is 541 million updates per second (MUPS) per processor only for spin updates, and it becomes 467 MUPS per processor for spin updates and CCF calculations at every step. We will see the simulation for four-dimensional hypercubic lattice later, and the performance is 397 MUPS only for update, and 355 MUPS for update and CCF calculation.
- ³⁵C. Michael, *Phys. Rev.* **33**, 7861 (1986).
- ³⁶N. Ito and Y. Kanada, *Supercomputer* **5**, 31 (1988).
- ³⁷N. Ito and Y. Kanada, *Proceedings of Supercomputing 1990, New York, 1990* (IEEE Computer Society, Los Alamitos 1990), p. 753.
- ³⁸N. Ito, M. Kikuchi, and Y. Okabe, *Int. J. Mod. Phys. C* **C4**, 569 (1993).
- ³⁹T.S. Lewis and W.H. Payne, *J. ACM* **20**, 456 (1973).
- ⁴⁰N. Ito and Y. Kanada, *Supercomputer* **7**, 29 (1990).
- ⁴¹It has been pointed out that there exists a dynamically singular phase, called the Griffiths phase, in this temperature region (Refs. 8,12, and 42). It is investigated that remarkable slow dynamics are suggested for the equilibrium autocorrelation function (2.11); nonexponential but faster than power-law decay. However, we do not examine this possibility in this paper, since, in the observation time in our nonequilibrium process, it is too short to detect the component of such a slow dynamics, which would have a small dynamical amplitude in the initial state, from other exponential components with large initial amplitude. Thus, we call this region the ‘PM’ phase.
- ⁴²R.B. Griffiths, *Phys. Rev. Lett.* **23**, 17 (1969).
- ⁴³It would be pointed out that tails of some curves in Fig. 1(c) curl up a little, e.g., for $t_w = 10^2$ and 10^3 . At a glance, this indicates a tendency of finite SG ordering for $t \rightarrow \infty$. However, we do not take it seriously and consider that this comes from numerical deviation appearing in a positive function decaying to zero. In fact, this effect appears as the rounding peak around the saturation ($t_w/t \ll 1$) in Fig. 3(c). Such a peak with the same order of deviation is also observed around the critical point Fig. 3(b), which should be numerical error because of the critical relaxation. Therefore, we expect that the rounding peak in Fig. 3(c) also comes from the numerical error.
- ⁴⁴Careful observation is necessary to see the decreasing behavior for $T < T_g$, since the data points of smaller t_w for $t_w/t > 1$ are too large and out of range in the figure. A universal curve is found for $t_w/t > 1$, which is monotonically decreasing with t_w/t . For each waiting time, $\lambda(t, t_w)$ is located on this curve for smaller t_w/t , while it is deviated with curling up for larger t_w/t . The deviation point of t_w/t is larger if t_w is larger. Therefore, if t_w/t is fixed, one can see the decreasing behavior of $\lambda(t, t_w)$.
- ⁴⁵N. Ito and M. Suzuki, *J. Phys. Soc. Jpn.* **60**, 1978 (1991).
- ⁴⁶N. Ito, *Computer-Aided Statistical Physics*, edited by C. -K. Hu, AIP Conf. Proc. **248** (AIP, New York, 1992).
- ⁴⁷The t_w dependence of the amplitude Eq. (5.4) is discussed. It is diverging with t_w because μ is positive. But it is not inconsistent with the fact that $|Q(t, t_w)| \leq 1$ because λ_{ne} is larger than μ .
- ⁴⁸R.E. Blundell, K. Humayun, and A.J. Bray, *J. Phys. A* **25**, L733 (1992).
- ⁴⁹D.A. Huse, *Phys. Rev. B* **40**, 304 (1989).